

---

# Polyphenols Profile, and In Vitro Antioxidant and Anticholinesterase Activities of Romanian Wild-Grown *Acer* spp. (*Sapindaceae*)

---

[Cornelia Bejenaru](#) , [Adina-Elena Segneanu](#) , [Ludovic Everard Bejenaru](#) \* , [Andrei Biță](#) , [Antonia Radu](#) , [George Dan Mogoșanu](#) , [Maria Viorica Ciocîlteu](#) , [Costel Valentin Manda](#)

Posted Date: 2 January 2025

doi: 10.20944/preprints202501.0083.v1

Keywords: *Acer* spp.; *Sapindaceae*; Romanian flora; phenolic acids; HPLC/UV/MS quantification; antioxidant activity; anticholinesterase activity



Preprints.org is a free multidisciplinary platform providing preprint service that is dedicated to making early versions of research outputs permanently available and citable. Preprints posted at Preprints.org appear in Web of Science, Crossref, Google Scholar, Scilit, Europe PMC.

Copyright: This open access article is published under a Creative Commons CC BY 4.0 license, which permit the free download, distribution, and reuse, provided that the author and preprint are cited in any reuse.

Article

# Polyphenols Profile, and In Vitro Antioxidant and Anticholinesterase Activities of Romanian Wild-Grown *Acer* spp. (*Sapindaceae*)

Cornelia Bejenaru <sup>1†</sup>, Adina-Elena Segneanu <sup>2†</sup>, Ludovic Everard Bejenaru <sup>3,\*</sup>, Andrei Biță <sup>3,†</sup>, Antonia Radu <sup>1</sup>, George Dan Mogoșanu <sup>3</sup>, Maria Viorica Ciocîlteu <sup>4</sup> and Costel Valentin Manda <sup>4</sup>

<sup>1</sup> Department of Pharmaceutical Botany, Faculty of Pharmacy, University of Medicine and Pharmacy of Craiova, 2 Petru Rareș Street, 200349 Craiova, Dolj County, Romania

<sup>2</sup> Institute for Advanced Environmental Research, West University of Timișoara (ICAM–WUT), 4 Oituz Street, 300086 Timișoara, Timiș County, Romania

<sup>3</sup> Department of Pharmacognosy & Phytotherapy, Faculty of Pharmacy, University of Medicine and Pharmacy of Craiova, 2 Petru Rareș Street, 200349 Craiova, Dolj County, Romania

<sup>4</sup> Department of Instrumental and Analytical Chemistry, Faculty of Pharmacy, University of Medicine and Pharmacy of Craiova, 2 Petru Rareș Street, 200349 Craiova, Dolj County, Romania

\* Correspondence: ludovic.bejenaru@umfcv.ro; Tel.: +40–351–443–507

† These authors contributed equally to this work.

**Abstract:** Our paper investigates for the first time, the polyphenols profile and in vitro antioxidant and anticholinesterase activities of the leaves and fruits of Romanian wild-grown *Acer* spp. (*Sapindaceae*): *A. campestre* L., *A. monspessulanum* L., *A. platanoides* L., *A. pseudoplatanus* L., *A. tataricum* L. High-performance liquid chromatography/ultraviolet/mass spectrometry (HPLC/UV/MS) technique was used for the identification and quantification of phenolic acids. The spectrophotometric method was applied for the assessment of total phenolic content (TPC), 2,2-diphenyl-1-picrylhydrazyl (DPPH), 2,2'-azino-bis(3-ethylbenzothiazoline-6-sulfonic acid) (ABTS) and ferric reducing antioxidant power (FRAP) antioxidant assays. In situ antioxidant properties were determined on high-performance thin-layer chromatography (HPTLC) plates after DPPH derivatization. Acetylcholinesterase inhibition effect was evaluated using microplate-based assay. Considering the polyphenols profile of *Acer* spp., our research highlights new natural resources with in vitro antioxidant and anticholinesterase activities.

**Keywords:** *Acer* spp.; *Sapindaceae*; Romanian flora; phenolic acids; HPLC/UV/MS quantification; antioxidant activity; anticholinesterase activity

## 1. Introduction

*Acer* genus (formerly *Aceraceae*, now classified under *Sapindaceae* family) includes trees, and more rarely shrubs, with opposite, long-petiolate, deciduous leaves that are typically palmately lobed (less commonly entire or pinnately compound). The flowers are often unisexual, greenish or yellowish, sometimes apetalous, actinomorphic, pentamerous, and arranged in inflorescences. The fruit is a double samara, with each of the two nutlets bearing a lateral, reticulately veined wing, which may be membranous or coriaceous [1–4]. *Acer* genus comprises 129 species distributed across the temperate regions of the Northern Hemisphere (Europe, North Africa, Asia, and North America) [1–6]. In Europe, 15 species are found, and five are native to Romania (*A. campestre* L., *A. monspessulanum* L., *A. platanoides* L., *A. pseudoplatanus* L., *A. tataricum* L.) [1–4]. Most *Acer* spp. are found in China, where there are 99 species, of which 61 are endemic [5,6]. The name of the *Acer* genus originates from the Latin word meaning “hard”, referring to the strength of the wood of these plants [1]. In Romania, *Acer* spp. are commonly referred to as “Arțar”, “Paltin”, or “Jugastru”. The popular names for the

five native species in Romania are as follows: *A. campestre* L. – Field Maple (Jugastru); *A. monspessulanum* L. – Banat Field Maple (Jugastru de Banat); *A. platanoides* L. – Norway Maple (Arțar, Paltin de câmp); *A. pseudoplatanus* L. – Sycamore Maple (Paltin, Paltin de munte); *A. tataricum* L. – Tatar Maple (Arțar tătarăsc, Gladiș) [1–4].

*Acer* spp. are utilized in traditional medicine, in the food industry (notably for producing maple syrup as a sweetener), in constructions, and as ornamental plants (valued for their foliage shape and color) or for street planting [5–8]. In traditional medicine across East Asia, Europe, and North America, 40 species and 11 subspecies of *Acer* genus are used to treat hypertension, indigestion, as anti-inflammatory agents, and for arthralgia, rheumatism, sore throat, pneumonia, liver and eye diseases, and as emetics [5,6]. In traditional Chinese medicine, more than 20 *Acer* spp. are employed for therapeutic purposes [5,6]. In northeastern Asia, particularly Japan and Korea, several *Acer* spp. have been used for years in traditional medicine, including *A. maximowiczianum* Miq., *A. pictum* Thunb., *A. pycnanthum* K. Koch, and *A. tegmentosum* Maxim. [5]. In Japan, *A. pycnanthum* has been used for eye care, while in Korea, *A. tegmentosum* was utilized to treat liver conditions such as hepatitis, cirrhosis, and even hepatic cancer, as well as traumatic hemorrhages [5,8]. In China, *A. truncatum* Bunge is recommended for angina pectoris and cerebrovascular diseases, whereas *A. ginnala* Maxim. is used for acute diarrhea and tonsillopharyngitis [5,8–10]. In Europe, *Acer* spp. are less studied and known for their medicinal properties. Therapeutic formulations derived from *Acer* spp. include extracts made from roots, bark, leaves, flowers, and fruits [5–10].

The chemical composition of plants in the *Acer* genus includes over 331 compounds identified in 34 species, encompassing flavonoids, tannins, diarylheptanoids, phenylpropanoid derivatives, terpenoids, phytosterols, as well as benzoic acid derivatives, alkaloids, carbohydrates, fatty acids, amino acids, vitamins, and minerals [5,9,10]. Flavonoids, found in leaves and/or branches, are the primary components, with more than 62 compounds identified across 21 species. These include flavan-3-ols, flavanonols, anthocyanidins, flavones, flavanones, isoflavones, and chalcones. The main aglycones of these compounds are kaempferol, quercetin, myricetin, apigenin, luteolin, naringenin, and isorhamnetin [5,9]. A total of 41 tannin compounds have been identified, the majority being gallic (hydrolysable) tannins, along with five ellagitannins and four condensed tannins [5,6,11,12]. The known phenylpropanoid derivatives total 74, classified based on their structure into simple phenylpropanoids, lignans, or coumarins [5,6,13]. Fatty acids have been identified in the seed oil of *Acer* spp., such as *A. monspessulanum* [14], *A. platanoides*, *A. pseudoplatanus* [15], *A. truncatum* [16–18], with  $\gamma$ -linolenic acid playing a significant role among omega-6 fatty acids.

The pharmacological actions of *Acer* spp. have been increasingly studied over the past 20 years, utilizing various types of extracts, preparations, or natural compounds [5]. Reported activities include hepatoprotective [5,10,11,19], antioxidant [5,11,20–22], anti-inflammatory [5,11,23–25], neuroprotective [5,26,27], antiproliferative [5,11,20,28–30], estrogen-like [5,31,32], bone protective [5,33], antimicrobial [5,20,34], hypoglycemic [5,35], anti-obesity [5,11,19,27,36–38], anti-tyrosinase and anti-melanogenic [5,11,39], skin protective and anti-photoaging [5,11,40–42]. Additionally, studies have been conducted to explore the correlation between chemical structure and pharmacological activity [5].

Current data have highlighted aspects of the chemical composition and pharmacological actions of the five *Acer* spp. that spontaneously grow in Romania. However, the majority of studies in recent years have focused on *A. truncatum*, a species native to northern China, traditionally used for treating cardiovascular diseases. Due to its beneficial properties, it has been introduced to East Asia, Europe, and North America. Studies on *A. truncatum* have confirmed its antioxidant, antimicrobial, antitumor, anti-inflammatory, and neuroprotective properties [8,13,16–18,35,36,43–47]. Additionally, two subspecies of *A. tataricum* (subsp. *ginnala* and subsp. *theiferum*) have been studied for their antioxidant activity, attributed to their rich polyphenol content. The leaves and branches of these subspecies are used to prepare a tea consumed in China as a green tea substitute [48].

Due to their content in toxic dipeptides such as hypoglycin A (HGA), hypoglycin B (HGB), methylenecyclopropylglycine (MCPPrG) and  $\gamma$ -glutamyl-MCPPrG, *Acer* spp. (e.g., *A. pseudoplatanus*) are responsible for some cases of herbivore poisoning [49,50].

Our paper aimed to investigate, for the first time, the content of phenolic acids in leaves and fruits from *Acer* spp., which grow spontaneously in Romania, collected from the southwestern region, along with their antioxidant and acetylcholinesterase (AChE) inhibitory activities. Also, the research provides entirely new data in the context of understanding *Acer* spp. from a therapeutic perspective.

## 2. Materials and Methods

### 2.1. Plant Material

The leaves and fruits of wild-grown *Acer* spp. species were collected during the summer period (June–July 2024) from southwest Romania flora (Oltenia Region). All vegetal samples for analysis were deposited in the Herbarium of the Department of Pharmaceutical Botany, Faculty of Pharmacy, University of Medicine and Pharmacy of Craiova. The air-dried plant material was stored in brown paper bags for 24 hours in a cool and dark place at room temperature (RT) until processing for extraction and analysis. The research did not involve endangered or protected species.

In this study, the samples were denoted using a systematic notation to represent different species of the *Acer* genus and their respective plant parts. This notation facilitated a clear and organized reference to the specific plant species and parts analyzed in the experiments (Table 1).

**Table 1.** Sample coding of plant material.

Sample	Species / vegetal product	Date / site of collection (southwest Romania flora)	Voucher specimen
A1	<i>A. pseudoplatanus</i> / folium	1 July 2024 / Craiova City, Dolj County	ACER-PPT-2024-0701
A2	<i>A. tataricum</i> / folium	12 June 2024 / Craiova City, Dolj County	ACER-TAT-2024-0612
A3	<i>A. tataricum</i> / fructus		
A4	<i>A. campestre</i> / folium	12 June 2024 / Craiova City, Dolj County	ACER-CAM-2024-0612
A5	<i>A. campestre</i> / fructus		
A6	<i>A. pseudoplatanus</i> / fructus	1 July 2024 / Craiova City, Dolj County	ACER-PPT-2024-0701
A7	<i>A. platanoides</i> / folium	7 July 2024 / Craiova City, Dolj County	ACER-PLT-2024-0707
A8	<i>A. platanoides</i> / fructus		
A9	<i>A. monspessulanum</i> / folium	21 July 2024 / Dubova Village, Mehedinți County	ACER-MON-2024-0721
A10	<i>A. monspessulanum</i> / fructus		

### 2.2. Chemicals and Reagents

A variety of high-purity solvents and reagents were employed throughout the experimental procedures to ensure precise and reliable outcomes. The solvents used included ethanol, methanol, acetonitrile, toluene, ethyl acetate (Merck, Darmstadt, Germany). Ultrapure water was produced using the HALIOS 12 lab water system (Neptec, Montabaur, Germany), providing the necessary purity for all aqueous solutions and dilutions. Additionally, formic acid (Merck) was utilized as an additive to enhance the performance of the mobile phases in high-performance liquid chromatography (HPLC) analysis.

Reagents for specific assays and analytical procedures were carefully selected to support the experimental goals. These included Folin–Ciocalteu reagent, sodium carbonate, 2,2-diphenyl-1-picrylhydrazyl (DPPH), 2,2'-azino-bis(3-ethylbenzothiazoline-6-sulfonic acid) (ABTS), potassium persulfate, acetate buffer, 2,4,6-tris(2-pyridyl)-1,3,5-triazine (TPTZ), ferric chloride (FeCl<sub>3</sub>), ferrous

sulfate heptahydrate ( $\text{FeSO}_4 \cdot 7\text{H}_2\text{O}$ ), hydrochloric acid (HCl) (Sigma-Aldrich, Taufkirchen, Germany). The reagents were tailored for the determination of total phenolic content (TPC), antioxidant activity, and enzymatic assays.

In the AChE inhibition assay, key reagents comprised 1-naphthyl acetate, Fast Blue B salt, and rivastigmine (Sigma-Aldrich), which served as a positive control.

For HPLC analysis, a comprehensive set of phenolic acid standards, including caffeic acid, chlorogenic acid, *p*-coumaric acid, ferulic acid, gallic acid, protocatechuic acid, syringic acid, and vanillic acid (Merck Millipore), was used for calibration and compound identification.

High-performance thin-layer chromatography (HPTLC) Silica gel 60 F<sub>254</sub>, 20×10 cm glass plates were purchased from Merck.

### 2.3. Sample Preparation

The extraction of plant material was performed using an ultrasound-assisted extraction (UAE) method with 70% ethanol as the solvent. A precise quantity of 0.1 g of finely powdered plant material was mixed with 10 mL of the ethanol solution in a suitable container. This mixture was subjected to ultrasonic treatment using a Bandelin Sonorex Digiplus DL 102H ultrasound bath (Bandelin electronic GmbH & Co. KG, Berlin, Germany – power 100 W; frequency 35 kHz) for 20 minutes at a controlled temperature of 50°C. The ultrasonic waves disrupted the plant cell walls, facilitating the release of bioactive compounds into the solvent. Post-extraction, the solution was filtered using a 0.22 µm syringe filter with a WWPTFE membrane (Acrodisc, Pall Corporation, Port Washington, NY, USA) to separate the liquid extract from the solid residue. The resulting extract was utilized for determining total polyphenol content as well as conducting antioxidant and neuroprotection assays.

For the HPLC analysis, 2 mL of the extract was dried under a gentle nitrogen stream to remove the solvent. The dried material was reconstituted with a solvent mixture of water and acetonitrile (9:1, *v/v*) to ensure compatibility with the HPLC mobile phase system. This step optimized the dissolution of bioactive compounds for chromatographic separation and detection. The reconstituted solution was filtered through a 0.22 µm syringe filter before injection into the HPLC system.

### 2.4. Preparation of Standards

Standards for the HPLC analysis included eight phenolic acids: caffeic acid, chlorogenic acid, *p*-coumaric acid, ferulic acid, gallic acid, protocatechuic acid, syringic acid, and vanillic acid. These standards were prepared as stock solutions at a concentration of 1 mg/mL using methanol. Serial dilutions were then made to achieve calibration concentrations ranging from 0.1 µg/mL to 50 µg/mL. A volume of 10 µL was injected into the HPLC system for both standards and samples.

### 2.5. Total Phenolic Content Assay

TPC was determined by loading 20 µL of the plant extract into a 96-well microplate, followed by the addition of 100 µL of Folin–Ciocalteu reagent. After mixing for three minutes, 80 µL of a 4% sodium carbonate solution was added, and the mixture was stirred for another three minutes. The plate was incubated in the dark for two hours to allow the reaction to develop. Absorbance was measured at 620 nm using a FLUOstar Optima microplate reader (BMG Labtech, Ortenberg, Germany). Gallic acid was used to prepare a standard curve, with calibration solutions ranging from 5 mg/mL to 625 µg/mL. All measurements were performed in triplicate.

### 2.6. DPPH Antioxidant Assay

For the DPPH assay, 50 µL of each sample was added to a 96-well microplate, followed by serial dilutions to obtain a range of decreasing concentrations. 150 µL solution of 0.2 mM DPPH in ethanol was then added. The mixtures were incubated in the dark for 30 minutes at RT, and absorbance was measured at 517 nm using a FLUOstar Optima microplate reader. Antioxidant activity was quantified by calculating the half maximal inhibitory concentration (IC<sub>50</sub>) value, representing the sample

concentration required to inhibit 50% of the DPPH free radicals. All analyses were performed in triplicate.

### 2.7. ABTS Antioxidant Assay

ABTS assay involved the addition of 50  $\mu\text{L}$  of sample to a 96-well microplate. Serial dilutions were prepared similar to the previous antioxidant assay, and then 150  $\mu\text{L}$  of the ABTS solution (a mixture of 7.4 mM ABTS and 2.6 mM potassium persulfate) was added. After six minutes, the absorbance was measured at 620 nm using a FLUOstar Optima microplate reader. The  $\text{IC}_{50}$  value, indicating the concentration needed to inhibit 50% of ABTS radicals, was determined from a dose-response curve. Samples were tested in triplicate.

### 2.8. FRAP Antioxidant Assay

For the ferric reducing antioxidant power (FRAP) assay, the reagent was prepared by combining acetate buffer (pH 3.6), 10 mM TPTZ solution in 40 mM HCl, and 20 mM  $\text{FeCl}_3$  solution. A calibration curve was generated using  $\text{Fe}^{2+}$  standards ranging from 65  $\mu\text{mol/L}$  to 500  $\mu\text{mol/L}$ . In each assay, 10  $\mu\text{L}$  of the sample or standard was added to a 96-well microplate with 190  $\mu\text{L}$  of the freshly prepared FRAP reagent. Reaction mixtures were incubated for 30 minutes at RT, and absorbance was measured at 595 nm. Results were expressed as  $\mu\text{mol Fe}^{2+}$  equivalents. All samples were analyzed in triplicate.

### 2.9. Acetylcholinesterase Inhibition Assay

The evaluation of AChE inhibitory activity was conducted using a detailed microplate-based assay to determine the inhibitory potential of the tested samples.

Each sample was serially diluted directly on a 96-well microplate to generate a range of concentrations for the analysis. Starting with an initial volume of the stock solution, serial dilutions were performed to ensure the final volume in each well was precisely 50  $\mu\text{L}$ . This systematic approach allowed for a detailed evaluation of the inhibitory effects across varying sample concentrations. To each well containing 50  $\mu\text{L}$  of the samples, 50  $\mu\text{L}$  of 1-naphthyl acetate solution (3 mg/mL in ethanol) was added. This substrate serves as a reactant in the enzymatic reaction catalyzed by AChE. Following the addition of the substrate, 150  $\mu\text{L}$  of AChE solution (3.33 U/mL) was carefully introduced into each well. This step initiated the enzymatic reaction, producing measurable products that reflect enzyme activity. To enable visualization of the reaction and quantify enzyme activity, 50  $\mu\text{L}$  of Fast Blue B salt solution (3 mg/mL in water) was added to the wells. This reagent reacts with the enzymatic products, generating a distinct color that correlates with AChE activity.

Rivastigmine, a recognized AChE inhibitor, was prepared at a concentration of 1 mg/mL in methanol and included in the assay as a positive control. This ensured a reliable reference point for evaluating the inhibitory potential of the test samples.

Absorbance was measured at 595 nm using a FLUOstar Optima microplate reader. The data collected was analyzed to calculate the  $\text{IC}_{50}$  value for each sample, representing the concentration required to inhibit 50% of AChE activity.

### 2.10. HPTLC–DPPH Fingerprint

All ethanolic extracts were applied as 8  $\mu\text{L}$ , 8-mm bands on HPTLC plates using a CAMAG Linomat 5 applicator (CAMAG, Muttenz, Switzerland). The HPTLC plates were developed in a twin trough chamber using a solvent mixture of toluene–ethyl acetate–formic acid (6:6:1, *v/v/v*) up to a migration distance of 90 mm. After development, the HPTLC plates were dried using a hair dryer for five minutes. The plates were then documented under ultraviolet (UV) light at 254 nm and 365 nm without derivatization, and under white light after DPPH derivatization (0.05% DPPH reagent in methanol), to visualize the antioxidant activity. Caffeic acid, chlorogenic acid, *p*-coumaric acid, gallic acid and protocatechuic acid standards were added as 2  $\mu\text{L}$  bands each of a 1 mg/mL concentration.

### 2.11. HPLC/UV/MS Analysis

HPLC analysis was conducted using a Waters Acquity Arc system equipped with a photodiode array (PDA) detector and a QDa mass detector. Chromatographic separation was performed using a CORTECS C18 column (4.6×50 mm, 2.7 µm particle size) maintained at 30°C. Mobile phases included water with 0.01% formic acid (A) and acetonitrile with 0.01% formic acid (B). The HPLC gradient method began with a mobile phase composition of 99% A, at a constant flow rate of 0.8 mL/min. This initial condition was held for one minute. From one to 13 minutes, the proportion of mobile phase A decreased to 70%. At 13.10 minutes, the mobile phase composition remained steady at 70% A. Subsequently, from 13.60 to 17.60 minutes, the composition shifted to 20% A, which was maintained for column cleaning and to remove any strongly retained compounds. After this phase, at 18.10 minutes, the mobile phase returned to the initial condition of 99% A, and this composition was held until 21.10 minutes for re-equilibration and preparation for the next injection. Between each injection, the column was equilibrated for 10 minutes to ensure stability and reproducibility. Samples were maintained at 8°C during the analysis to preserve their integrity.

Quantification was carried out at 265 nm for gallic acid, protocatechuic acid, vanillic acid, and syringic acid, and at 325 nm for chlorogenic acid, caffeic acid, *p*-coumaric acid, and ferulic acid, while mass confirmation was performed using specific mass-to-charge ratios (*m/z*). These included protocatechuic acid (*m/z* 153), *p*-coumaric acid (*m/z* 163), vanillic acid (*m/z* 167), gallic acid (*m/z* 169), caffeic acid (*m/z* 179), ferulic acid (*m/z* 193), syringic acid (*m/z* 197), and chlorogenic acid (*m/z* 353).

### 2.12. Statistical Analysis

Statistical analyses were performed to evaluate the relationships between phenolic compounds, TPC, antioxidant (DPPH, ABTS, FRAP) and AChE inhibitory activities. The Shapiro–Wilk test was applied to assess the normality of the data distribution, ensuring the appropriateness of subsequent parametric analyses. Pearson’s correlation coefficients were calculated to determine the strength and direction of linear relationships between the variables. To visualize and explore multivariate relationships and patterns among the measured variables, principal component analysis (PCA) was conducted. All statistical tests and analyses were performed using GraphPad Prism version 9.1.0, which provided comprehensive tools for normality testing, correlation analysis, and multivariate data exploration. Statistical significance was considered at a *p*-value threshold of less than 0.05 for all tests.

## 3. Results

### 3.1. Total Phenolic Content

TPC of the analyzed *Acer* samples ranged from 61.48±3.76 µg GAE/mL (A7 sample) to 512.8±20.54 µg GAE/mL (sample A2). Among the samples, A2 exhibited the highest TPC, followed by A3 with 456.1±16.94 µg GAE/mL, while A7 and A5 showed the lowest values, with 61.48±3.76 and 68.45±8.56 µg GAE/mL, respectively. Moderate TPC values were observed in samples such as A9 (251.8±19.06 µg GAE/mL) and A10 (193.8±8.93 µg GAE/mL). The variation in TPC across samples suggests significant diversity in the phenolic composition among *Acer* spp. The data are presented in Table 2 and illustrated graphically in Figure 1.

**Table 2.** TPC values (mean ± SD) of the analyzed *Acer* (A1–A10) samples.

Sample	TPC (µg GAE/mL)
A1	94.01±14.41
A2	512.8±20.54
A3	456.1±16.94
A4	225.8±5.527
A5	68.45±8.563
A6	91.04±3.572

A7	61.48±3.755
A8	164.1±4.978
A9	251.8±19.06
A10	193.8±8.927

GAE: Gallic acid equivalents; SD: Standard deviation; TPC: Total phenolic content.

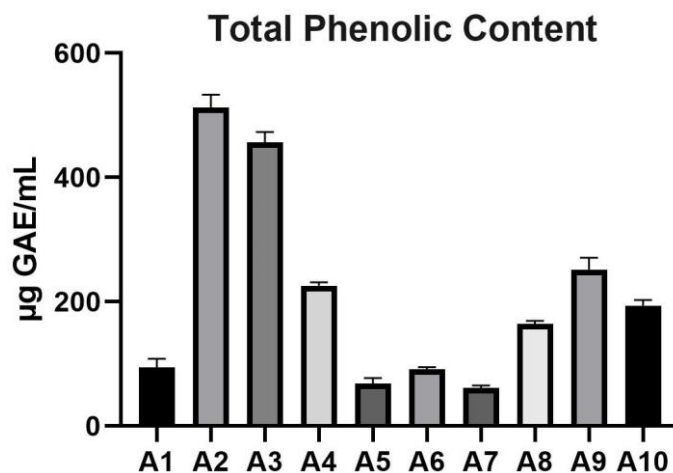


**Figure 1.** TPC of the analyzed *Acer* (A1–A10) samples. GAE: Gallic acid equivalents; TPC: Total phenolic content.

### 3.2. Antioxidant Activity

DPPH and ABTS antioxidant assays were used to assess the radical scavenging activities of the *Acer* samples, expressed as  $IC_{50}$  values ( $\mu\text{g/mL}$ ), where lower values indicate higher antioxidant activity. Sample A3 exhibited the highest antioxidant activity in both assays, with  $IC_{50}$  values of  $10.88\pm 3.39 \mu\text{g/mL}$  for DPPH and  $10.39\pm 2.86 \mu\text{g/mL}$  for ABTS. Sample A2 also showed strong antioxidant potential, with  $IC_{50}$  values of  $22.61\pm 3.28 \mu\text{g/mL}$  (DPPH) and  $15.68\pm 3.31 \mu\text{g/mL}$  (ABTS). In contrast, sample A7 had the weakest antioxidant activity, with  $IC_{50}$  values of  $290.2\pm 39.2 \mu\text{g/mL}$  (DPPH) and  $271.2\pm 60.7 \mu\text{g/mL}$  (ABTS). Moderate antioxidant activities were observed in samples such as A9 ( $54.25\pm 10.59 \mu\text{g/mL}$  for DPPH,  $37.75\pm 9.7 \mu\text{g/mL}$  for ABTS) and A10 ( $60.62\pm 12.72 \mu\text{g/mL}$  for DPPH,  $57.58\pm 13.61 \mu\text{g/mL}$  for ABTS). These results are highlighted in Table 3 and illustrated in Figure 2.

**Table 3.** Values (mean  $\pm$  SD) of in vitro antioxidant (DPPH, ABTS and FRAP) assays for analyzed *Acer* (A1–A10) samples.

Sample	DPPH $IC_{50}$ ( $\mu\text{g/mL}$ )	ABTS $IC_{50}$ ( $\mu\text{g/mL}$ )	FRAP ( $\mu\text{mol Fe}^{2+}/\text{L}$ )
A1	137.4±51.9	132.5±27.3	117.8±7.659
A2	22.61±3.28	15.68±3.31	1119±164.6
A3	10.88±3.385	10.39±2.861	1158±48.98
A4	63.14±8.96	50.45±10.89	310.6±18.36
A5	226.9±32	212.7±63.3	154.4±9.225
A6	138.2±20.4	79.29±17.3	294.5±26.92
A7	290.2±39.2	271.2±60.7	139.8±5.361
A8	81.78±25.27	57.28±15.97	354.7±20.75
A9	54.25±10.59	37.75±9.7	471±12.87
A10	60.62±12.72	57.58±13.61	378.1±5.64

ABTS: 2,2'-Azino-bis(3-ethylbenzothiazoline-6-sulfonic acid); DPPH: 2,2-Diphenyl-1-picrylhydrazyl; FRAP: Ferric reducing antioxidant power;  $IC_{50}$ : Half-maximal inhibitory concentration.; SD: Standard deviation.

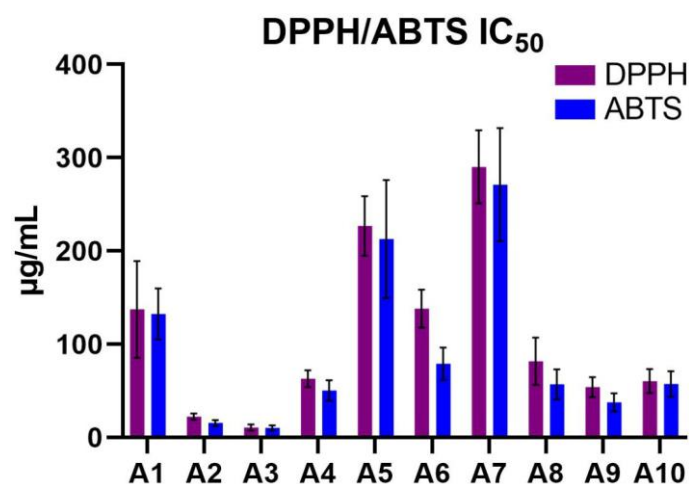


**Figure 2.** DPPH/ABTS IC<sub>50</sub> values of the analyzed *Acer* (A1–A10) samples. ABTS: 2,2'-Azino-bis(3-ethylbenzothiazoline-6-sulfonic acid); DPPH: 2,2-Diphenyl-1-picrylhydrazyl; IC<sub>50</sub>: Half-maximal inhibitory concentration.

FRAP assay, measured in  $\mu\text{mol Fe}^{2+}/\text{L}$ , revealed significant differences in antioxidant capacity among the *Acer* samples. Sample A2 demonstrated the highest reducing power at  $1119 \pm 164.6 \mu\text{mol Fe}^{2+}/\text{L}$ , followed closely by sample A3, with  $1158 \pm 48.98 \mu\text{mol Fe}^{2+}/\text{L}$ . Samples A9 ( $471 \pm 12.87 \mu\text{mol Fe}^{2+}/\text{L}$ ) and A10 ( $378.1 \pm 5.64 \mu\text{mol Fe}^{2+}/\text{L}$ ) exhibited moderate reducing capacities. In contrast, samples A1 ( $117.8 \pm 7.659 \mu\text{mol Fe}^{2+}/\text{L}$ ) and A7 ( $139.8 \pm 5.361 \mu\text{mol Fe}^{2+}/\text{L}$ ) displayed the lowest reducing power. These findings underscore substantial variability in the antioxidant potential of the *Acer* samples, as shown in Table 3 and depicted in Figure 3.

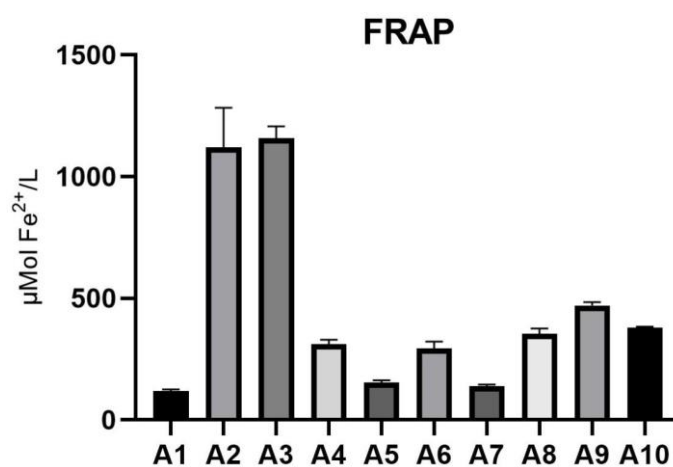


**Figure 3.** Results of the FRAP assay for *Acer* (A1–A10) samples. FRAP: Ferric reducing antioxidant power.

### 3.3. Acetylcholinesterase Inhibition Activity

AChE inhibition assay revealed that only two *Acer* samples, A2 and A3, demonstrated a positive inhibitory response. Sample A2 exhibited an IC<sub>50</sub> value of  $7.908 \pm 7.503 \text{ mg/mL}$ , while A3 showed a higher inhibitory activity with an IC<sub>50</sub> value of  $15.95 \pm 8.52 \text{ mg/mL}$ . These findings suggest that samples A2 and A3 possess potential AChE inhibitory properties, as presented in Figure 4.

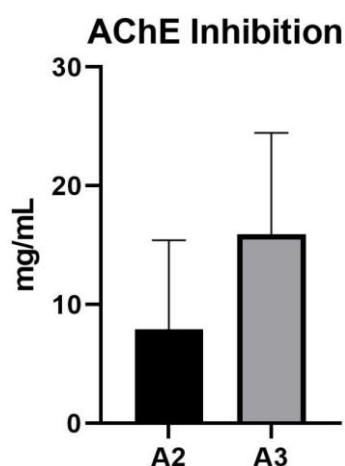


**Figure 4.** AChE inhibitory activity IC<sub>50</sub> values for *Acer* (A1–A10) samples. AChE: Acetylcholinesterase; IC<sub>50</sub>: Half-maximal inhibitory concentration.

### 3.4. HPTLC–DPPH Fingerprint

HPTLC fingerprint at 254 nm showed clear and distinct bands for all the standards, including caffeic acid ( $R_f$  0.51), chlorogenic acid ( $R_f$  0.033), *p*-coumaric acid ( $R_f$  0.58), gallic acid ( $R_f$  0.42), and protocatechuic acid ( $R_f$  0.50). The intensity of the bands was consistent, with all standards being well-visible under these conditions, indicating that this wavelength provides optimal visualization for detecting the tested phenolic compounds (Figure 5).

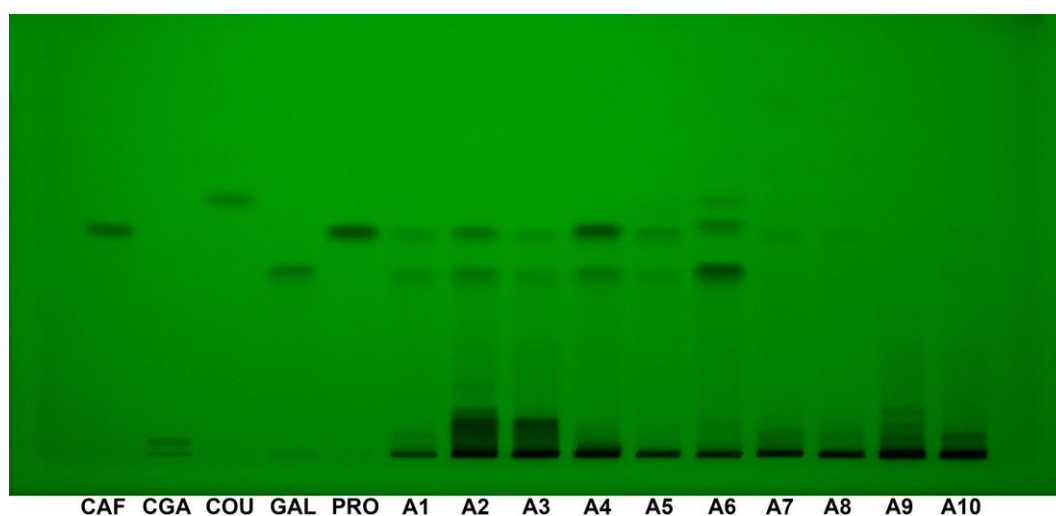


**Figure 5.** HPTLC fingerprint (254 nm, without derivatization) for *Acer* (A1–A10) samples and phenolic acids reference bands. CAF: Caffeic acid; CGA: Chlorogenic acid; COU: *p*-Coumaric acid; GAL: Gallic acid; HPTLC: High-performance thin-layer chromatography; PRO: Protocatechuic acid.

At 365 nm, the visibility of the standards varied significantly. While caffeic acid ( $R_f$  0.51) and chlorogenic acid ( $R_f$  0.033) exhibited clear and prominent fluorescence, gallic acid ( $R_f$  0.42) and protocatechuic acid ( $R_f$  0.50) were not visible under this wavelength. *p*-Coumaric acid ( $R_f$  0.58) was faintly visible with very low fluorescence intensity, indicating a reduced ability to detect certain phenolic compounds under these conditions (Figure 6).

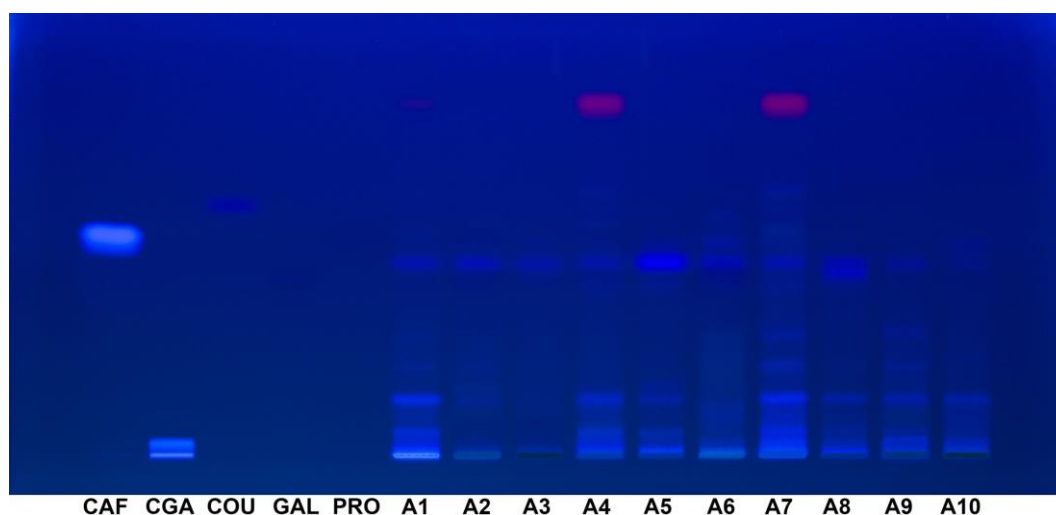


**Figure 6.** HPTLC fingerprint (365 nm, without derivatization) for *Acer* (A1–A10) samples and phenolic acids reference bands. CAF: Caffeic acid; CGA: Chlorogenic acid; COU: *p*-Coumaric acid; GAL: Gallic acid; HPTLC: High-performance thin-layer chromatography; PRO: Protocatechuic acid.

Under white light with DPPH staining, the standards demonstrated varying intensities of radical scavenging activity. Caffeic acid ( $R_f$  0.51), chlorogenic acid ( $R_f$  0.033), gallic acid ( $R_f$  0.42), and protocatechuic acid ( $R_f$  0.50) exhibited strong and distinct bands, indicative of high antioxidant activity. However, *p*-coumaric acid ( $R_f$  0.58) showed only a very faint band with low intensity compared to the other standards, suggesting a weaker radical scavenging response under these conditions (Figure 7).

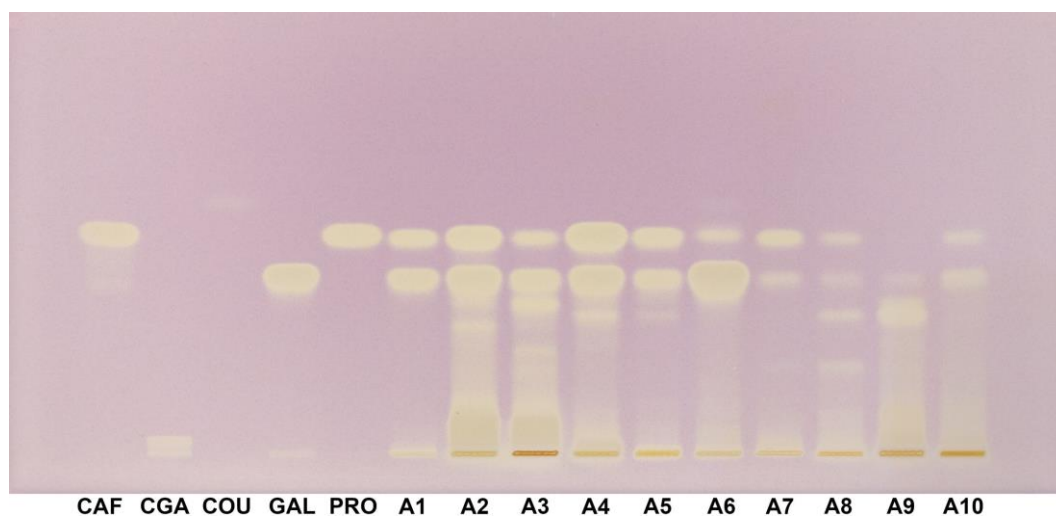


**Figure 7.** HPTLC–DPPH fingerprint (white light) for *Acer* (A1–A10) samples and phenolic acids reference bands. CAF: Caffeic acid; CGA: Chlorogenic acid; COU: *p*-Coumaric acid; DPPH: 2,2-Diphenyl-1-picrylhydrazyl; GAL: Gallic acid; HPTLC: High-performance thin-layer chromatography; PRO: Protocatechuic acid.

### 3.5. HPLC/UV/MS Analysis

HPLC analysis demonstrated effective separation and reproducibility of the compounds of interest under the selected parameters. The retention times for the identified compounds are presented in Table 4.

**Table 4.** Retention times for phenolic acids reference compounds.

Compound	$t_R$ (min)
Gallic acid	1.84

Compound	tr (min)
Protocatechuic acid	3.70
Chlorogenic acid	5.83
Vanillic acid	6.11
Caffeic acid	6.36
Syringic acid	6.64
<i>p</i> -Coumaric acid	7.80
Ferulic acid	8.54

tr: Retention time.

HPLC chromatograms for all samples were successfully obtained at both 265 nm and 325 nm, showing distinct peaks corresponding to the compounds of interest. These results highlight the reliability of the method for analyzing the target compounds across the samples (Figures 8 and 9).

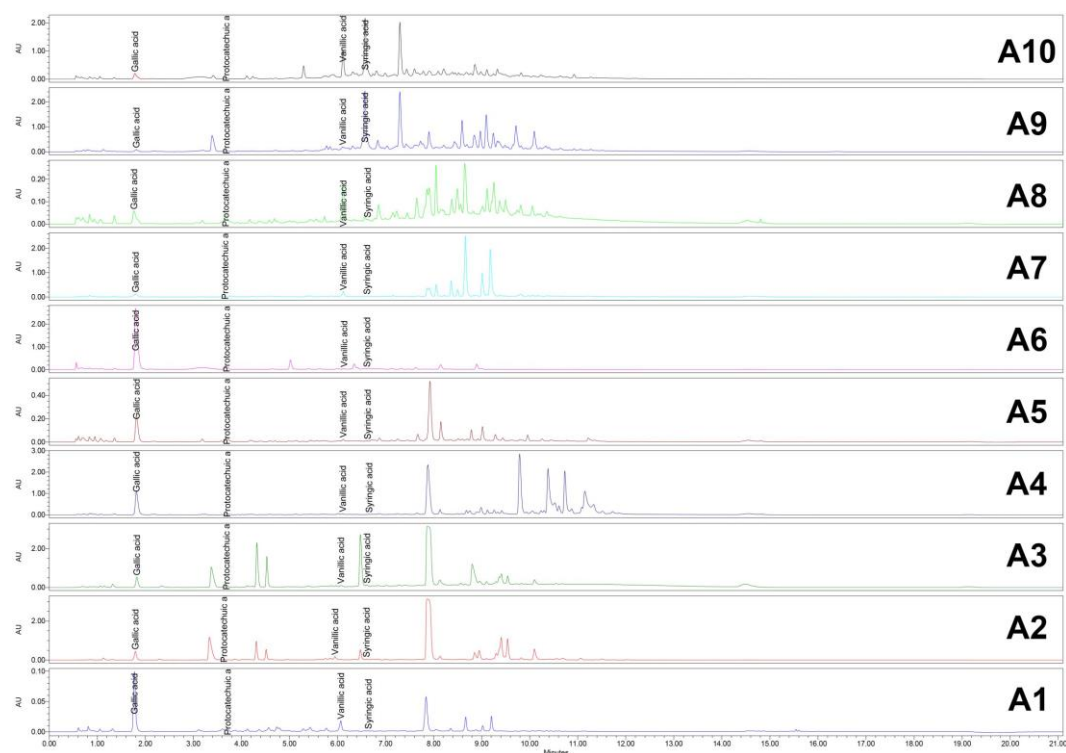


**Figure 8.** HPLC/UV (254 nm) chromatograms for *Acer* (A1–A10) samples. HPLC: High-performance liquid chromatography; UV: Ultraviolet.

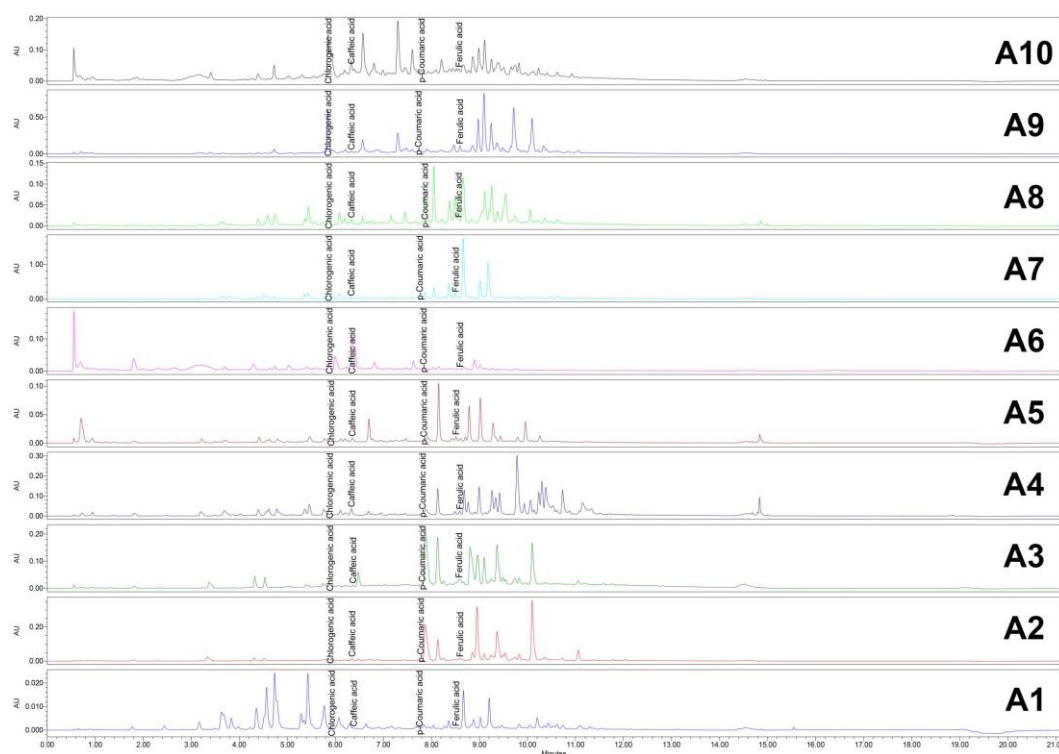


**Figure 9.** HPLC/UV (365 nm) chromatograms for *Acer* (A1–A10) samples. HPLC: High-performance liquid chromatography; UV: Ultraviolet.

The HPLC analysis revealed significant variability in the concentrations of phenolic acids across the *Acer* samples. Gallic acid was the most abundant compound in several samples, with the highest concentration observed in A6 ( $39.796 \pm 0.809$  mg/g). Protocatechuic acid also showed notable concentrations, particularly in samples A6 ( $6.219 \pm 0.227$  mg/g) and A3 ( $6.528 \pm 0.101$  mg/g). Chlorogenic acid exhibited the highest concentration in A9 ( $7.488 \pm 0.237$  mg/g), whereas syringic acid was most prominent in A10 ( $8.49 \pm 0.206$  mg/g). Vanillic acid levels were especially high in A10 ( $11.519 \pm 0.168$  mg/g), indicating its predominance in this sample. Caffeic acid and ferulic acid were present in lower concentrations overall, with their highest levels detected in A6 ( $1.323 \pm 0.019$  mg/g) and A7 ( $0.665 \pm 0.027$  mg/g), respectively. *p*-Coumaric acid was present in moderate amounts in most samples, with the highest concentration observed in A8 ( $1.401 \pm 0.016$  mg/g), followed by A7 ( $0.283 \pm 0.013$  mg/g). In contrast, syringic acid was detected in significantly higher amounts in A10 ( $8.49 \pm 0.206$  mg/g), making it the predominant compound in this sample. Other samples, such as A3 ( $0.82 \pm 0.017$  mg/g), also showed moderate levels of syringic acid, while lower levels were observed in the remaining samples (Table 5; Figure 10).

**Table 5.** Concentrations (mean  $\pm$  SD) of phenolic acids quantified in *Acer* (A1–A10) samples.

Sample	Caffeic acid (mg/g)	Chlorogenic acid (mg/g)	<i>p</i> -Coumaric acid (mg/g)	Ferulic acid (mg/g)	Gallic acid (mg/g)	Protocatechuic acid (mg/g)	Syringic acid (mg/g)	Vanillic acid (mg/g)
A1	$0.003 \pm 0.001$	$0.005 \pm 0.001$	$0.012 \pm 0.001$	$0.001 \pm 0.001$	$0.977 \pm 0.015$	$0.169 \pm 0.002$	$0.012 \pm 0.001$	$0.24 \pm 0.01$
A2	$0.122 \pm 0.004$	$0.114 \pm 0.004$	$0.024 \pm 0.001$	$0.109 \pm 0.005$	$4.75 \pm 0.205$	$1.171 \pm 0.021$	$0.459 \pm 0.007$	$2.076 \pm 0.036$
A3	$0.043 \pm 0.001$	$0.14 \pm 0.004$	$0.062 \pm 0.001$	$0.19 \pm 0.004$	$5.929 \pm 0.204$	$6.528 \pm 0.101$	$0.82 \pm 0.017$	$0.863 \pm 0.021$
A4	$0.35 \pm 0.009$	$0.07 \pm 0.002$	$0.158 \pm 0.002$	$0.08 \pm 0.002$	$14.05 \pm 0.473$	$1.04 \pm 0.012$	$0.081 \pm 0.002$	$0.436 \pm 0.007$
A5	$0.071 \pm 0.001$	$0.011 \pm 0.001$	$0.091 \pm 0.004$	$0.029 \pm 0.001$	$2.878 \pm 0.063$	$2.145 \pm 0.029$	$0.009 \pm 0.001$	$0.21 \pm 0.005$
A6	$1.323 \pm 0.019$	$0.302 \pm 0.009$	$0.227 \pm 0.002$	$0.01 \pm 0.001$	$39.796 \pm 0.809$	$6.219 \pm 0.227$	$0.154 \pm 0.003$	$0.173 \pm 0.005$
A7	$0.312 \pm 0.009$	$2.016 \pm 0.035$	$0.283 \pm 0.013$	$0.665 \pm 0.027$	$2.19 \pm 0.104$	$1.371 \pm 0.062$	$0.235 \pm 0.007$	$2.613 \pm 0.122$
A8	$0.105 \pm 0.001$	$0.239 \pm 0.004$	$1.401 \pm 0.016$	$0.025 \pm 0.001$	$0.94 \pm 0.024$	$2.304 \pm 0.048$	$0.091 \pm 0.003$	$2.167 \pm 0.052$
A9	$0.282 \pm 0.005$	$7.488 \pm 0.237$	$1.04 \pm 0.016$	$0.471 \pm 0.019$	$1.15 \pm 0.014$	$0.001 \pm 0$	$0.001 \pm 0$	$2.317 \pm 0.041$
A10	$0.622 \pm 0.006$	$1.648 \pm 0.07$	$0.412 \pm 0.015$	$0.061 \pm 0.002$	$2.926 \pm 0.119$	$2.459 \pm 0.031$	$8.49 \pm 0.206$	$11.519 \pm 0.168$

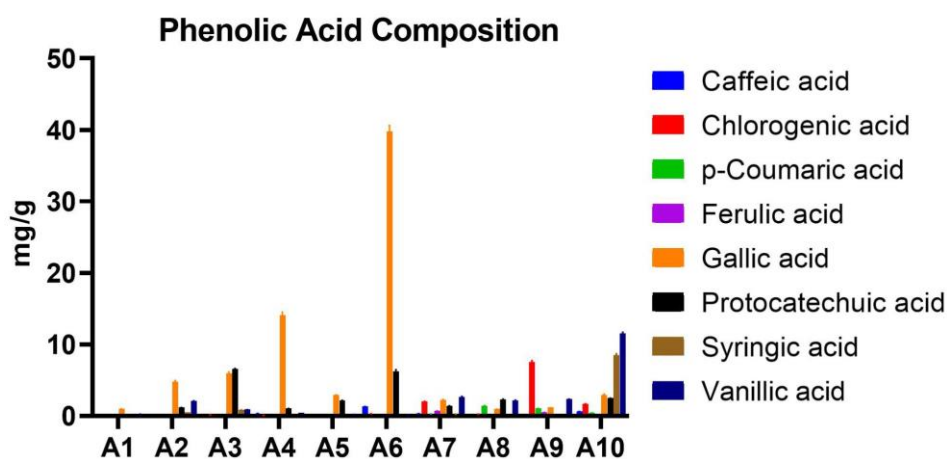


Figure 10. Phenolic acids quantified in analyzed *Acer* (A1–A10) samples.

## 4. Discussion

The relationship between TPC and the various activities, including in vitro antioxidant (DPPH, ABTS, and FRAP) and AChE inhibitory activities, reveals critical insights into the role of phenolics in bioactive processes. These activities provide a comprehensive understanding of the functional properties of phenolic compounds, particularly in their capacity to influence biological mechanisms [51–55].

We assessed the normality of the data using the Shapiro–Wilk test. The results indicated that all datasets followed a normal distribution, as they passed the normality test ( $p < 0.05$ ). This confirms the suitability of parametric statistical methods for further analysis.

### 4.1. Correlation of TPC with Antioxidant and AChE Inhibitory Activities

Antioxidant activities, as assessed through DPPH, ABTS, and FRAP assays, display significant correlations with TPC, underscoring the central role of phenolic compounds in determining radical scavenging capacity, reducing power, and overall antioxidant potential. DPPH assay, which measures free radical scavenging activity based on  $IC_{50}$  values, demonstrates a strong negative correlation with TPC ( $r = -0.787$ ,  $p = 0.007$ ). This finding suggests that higher TPC is associated with lower  $IC_{50}$  values, reflecting stronger antioxidant activity. This relationship can be attributed to the ability of phenolic compounds to donate electrons or hydrogen atoms, neutralizing free radicals effectively. Similarly, ABTS assay also reveals a strong negative correlation with TPC ( $r = -0.732$ ,  $p = 0.016$ ). Although DPPH and ABTS employ distinct radical systems, the consistent trends between the two assays reinforce the role of phenolic content as a critical determinant of antioxidant efficacy across varying methodologies.

FRAP assay, which evaluates reducing power, exhibits the strongest positive correlation with TPC ( $r = 0.969$ ,  $p < 0.0001$ ). This indicates that higher TPC contributes directly to an increased capacity to reduce  $Fe^{3+}$  ions to  $Fe^{2+}$  ions, a key indicator of reducing power. This robust correlation suggests that phenolic compounds, through their hydroxyl groups, serve as potent electron donors, thereby enhancing the antioxidant potential of the samples. Among the antioxidant activities, the FRAP assay's relationship with TPC highlights the pivotal role of phenolics in governing reducing power.

In addition to antioxidant activity, TPC also correlates significantly with anti-AChE activity, as assessed by AChE  $IC_{50}$  values. The positive correlation between TPC and AChE inhibitory activity ( $r = 0.818$ ,  $p = 0.004$ ) reflects the contribution of phenolic compounds to the inhibition of AChE, an enzyme associated with neurodegenerative disorders like Alzheimer's disease. Phenolic compounds are known to interact with cholinesterase enzymes through various mechanisms, including hydrogen bonding, hydrophobic interactions, and  $\pi$ - $\pi$  stacking. This finding underscores the dual role of phenolic content in contributing not only to antioxidant properties but also to neuroprotective effects.

The correlation between TPC and AChE inhibitory activity suggests that phenolics play a central role in modulating enzyme activity, further reinforcing their multifunctional bioactivity [56].

The interrelationships among the activities themselves provide additional evidence of the importance of TPC in driving biological efficacy. For example, the strong correlation between DPPH and ABTS activities ( $r=0.983$ ,  $p<0.0001$ ) reflects overlapping mechanisms of radical scavenging facilitated by phenolic compounds, while the significant relationship between FRAP and anti-AChE activities ( $r=0.902$ ,  $p=0.00036$ ) highlights the interconnectedness between reducing power and enzyme inhibition. This interplay suggests that phenolic compounds influence these activities through shared biochemical pathways, making TPC a comprehensive marker of their bioactive potential.

Overall, these findings emphasize the critical role of TPC in determining the antioxidant and anti-AChE activities of phenolic-rich samples. The strong correlations between TPC and these bioactivities underscore its importance as a predictor of functional properties, with higher TPC levels associated with enhanced biological efficacy [56]. These insights have significant implications for the development and application of natural products, particularly in therapeutic contexts where antioxidant and neuroprotective properties are desired. By optimizing phenolic content during extraction or processing, the bioactive potential of plant-derived products can be maximized, offering promising avenues for managing oxidative stress and neurodegenerative diseases. This relationship between TPC and biological activities highlights the centrality of phenolic compounds in contributing to health-promoting properties and the potential for their targeted utilization in functional food and pharmaceutical formulations.

#### 4.2. Correlation of Phenolic Acids with TPC, Antioxidant and AChE Inhibitory Activities

The lack of significant correlations between the quantified phenolic compounds and the measured activities (DPPH, ABTS, FRAP, and anti-AChE) or TPC suggests that the biological activities and overall phenolic content are not solely attributable to the individual compounds analyzed. This is further supported by the HPTLC–DPPH fingerprint, which reveals the presence of more intense antioxidant zones beyond those corresponding to the reference compounds quantified in this study. These findings indicate that other phenolic compounds, not quantified here, or synergistic interactions among various bioactive constituents likely play a pivotal role in determining the observed activities and TPC. The structural diversity and specific properties of the quantified phenolics may not fully align with the mechanisms assessed in the antioxidant and anticholinesterase assays, further explaining the lack of correlation. This underscores the complexity of natural extracts, where the overall activity often arises from the collective influence and synergistic interactions of multiple compounds, rather than the isolated effects of individual phenolics. The HPTLC–DPPH results highlight the importance of considering the entire phenolic profile and unquantified compounds when evaluating the bioactive potential of plant-based samples [51,52,54].

PCA biplot provides valuable insights into the relationships between phenolic compounds, antioxidant (DPPH, ABTS, FRAP) and anti-AChE activities, and TPC. By illustrating how these variables group and align across two principal components, PCA plot complements the Pearson's correlation analysis and highlights patterns of association that may not be immediately evident from numerical correlations alone (Figure 11).

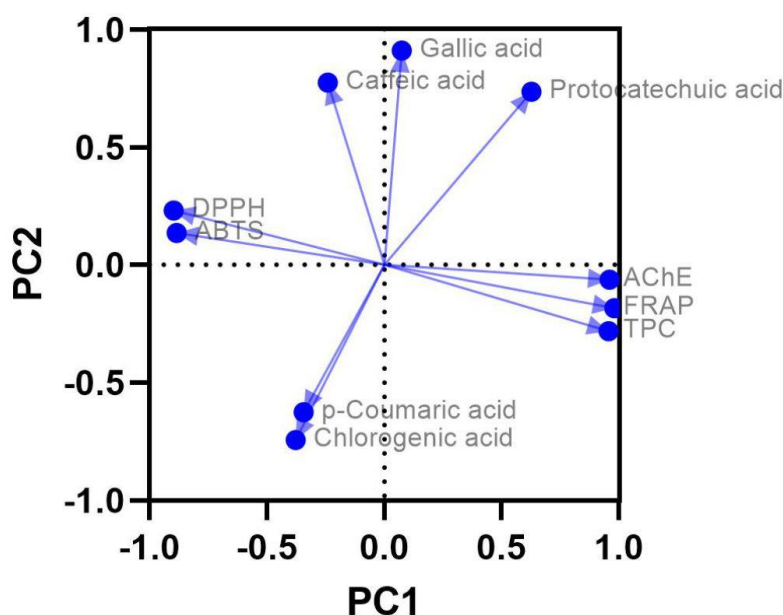


**Figure 11.** PCA highlights the relationships between phenolic acids content, TPC, antioxidant (DPPH, ABTS, FRAP) and AChE inhibitory activities. ABTS: 2,2'-Azino-bis(3-ethylbenzothiazoline-6-sulfonic acid; AChE: Acetylcholinesterase; DPPH: 2,2-Diphenyl-1-picrylhydrazyl; FRAP: Ferric reducing antioxidant power; PCA: Principal component analysis; TPC: Total phenolic content.

In the PCA plot, gallic acid, caffeic acid, and protocatechuic acid are positioned positively along the first principal component (PC1), which is closely aligned with AChE inhibitory, FRAP, and TPC assays. This grouping suggests that these compounds contribute to the activities associated with this axis. However, when examining the Pearson's correlation for gallic acid and TPC, the value is weakly negative ( $r=-0.154$ ,  $p=0.67$ ), indicating that gallic acid's contribution to TPC is either negligible or slightly antagonistic. This apparent contradiction can be explained by the overall complexity of interactions among the phenolic compounds and other bioactive constituents, as the PCA represents collective variance rather than individual direct correlations.

PCA also shows that DPPH and ABTS activities, which are represented as  $IC_{50}$  values, are located on the negative side of PC1, opposite to TPC, FRAP, and AChE inhibitory activities. This positioning reflects the inverse relationships between DPPH and ABTS with TPC, as confirmed by the strong negative Pearson's correlations (DPPH,  $r=-0.787$ ,  $p=0.007$ ; ABTS,  $r=-0.732$ ,  $p=0.016$ ). These findings underscore the fact that higher TPC, which correlates positively with FRAP and anti-AChE activity, is associated with lower  $IC_{50}$  values for DPPH and ABTS, indicating stronger radical scavenging activity.

Chlorogenic acid and *p*-coumaric acid, on the other hand, are positioned negatively along PC1 and show limited alignment with TPC, FRAP, and AChE inhibitory assays. This visual separation is consistent with their weak or negligible Pearson's correlations with these activities, reflecting their minor or indirect roles in contributing to overall bioactivity. Additionally, the proximity of protocatechuic acid to TPC and anti-AChE activity in the PCA plot highlights its moderate influence on these activities, even though its Pearson's correlations with TPC ( $r=0.16$ ,  $p=0.66$ ) and AChE inhibitory ( $r=0.521$ ,  $p=0.12$ ) assays do not reach statistical significance.

Overall, the PCA plot visually reinforces the strong interrelationships among TPC, FRAP, and anti-AChE assays, which are tightly clustered in the same quadrant, suggesting overlapping mechanisms of action and shared contributions to bioactivity. At the same time, the inverse placement of DPPH and ABTS relative to TPC and FRAP reflects their distinct role as measures of radical scavenging activity, inversely related to total phenolics. The PCA also reveals the varying contributions of individual phenolic compounds to these activities, emphasizing the complexity of interactions within the phenolic matrix and the need to consider both individual and collective effects of bioactive compounds. These findings highlight the multidimensional nature of phenolic-driven

activities and the importance of exploring their combined effects rather than focusing solely on individual compounds.

#### 4.3. Study Limitation

A limitation of the present study, which will be addressed in future work, is the analysis and correlation with more polar compounds, such as flavonoids. This is particularly evident from the HPTLC chromatogram, where compounds with higher affinity for the stationary phase and lower  $R_f$  values were not quantified or correlated with the measured activities. These polar compounds may play a significant role in the observed bioactivities, including antioxidant and anticholinesterase effects. Additionally, screening for compounds with potential AChE inhibitory activity directly on the HPTLC plate, similar to the DPPH assay used for antioxidant detection, represents another avenue for extending the study. These efforts will provide a more comprehensive understanding of the phenolic profile and its contributions to the observed biological activities [51].

## 5. Conclusions

For the first time, research on Romanian wild-grown *Acer* spp. highlights the relationships between phenolic compounds, antioxidant activities, anticholinesterase activity, and TPC. While TPC exhibited strong correlations with FRAP and AChE inhibitory activities, the quantified phenolic compounds showed limited individual contributions, suggesting the involvement of unquantified polar compounds and potential synergistic effects. These findings emphasize the complexity of *Acer* spp. extracts and the need for a broader analysis of bioactive constituents, including flavonoids and HPTLC-based activity screening, to fully understand their functional roles. Future studies will address these limitations to provide a deeper understanding of the bioactive potential of *Acer* spp.

**Author Contributions:** Conceptualization, C.B., A.E.S. and C.V.M.; methodology, L.E.B. and A.B.; validation, A.E.S., A.B. and M.V.C.; investigation, A.E.S., A.B., A.R. and M.V.C.; data curation, G.D.M. and C.V.M.; writing—original draft preparation, L.E.B., A.B. and G.D.M.; writing—review and editing, A.B. and G.D.M.; supervision, C.B., A.E.S. and L.E.B. All authors have read and agreed to the published version of the manuscript.

**Funding:** This research received no external funding.

**Institutional Review Board Statement:** Not applicable.

**Informed Consent Statement:** Not applicable.

**Data Availability Statement:** The original contributions presented in this study are included in the article. Further inquiries can be directed to the corresponding author.

**Conflicts of Interest:** The authors declare no conflicts of interest.

## References

1. Săvulescu, T.; Nyarady, E.I. (Eds). *Flora R.P.R.*, 1st ed.; Romanian Academy Publishing House: Bucharest, Romania, 1958; Volume VI, pp. 220–248 (in Romanian).
2. Tutin, T.G.; Heywood, V.H.; Burges, N.A.; Moore, D.M.; Valentine, D.H.; Walters, S.M.; Webb, D.A. (Eds). *Flora Europaea. Vol. 2: Rosaceae to Umbelliferae*, 1st ed.; Cambridge University Press: Cambridge, UK, 1968; pp. 237–239.
3. Ciocârlan, V. *Flora ilustrată a României. Pteridophyta et Spermatophyta*, 3rd ed.; Ceres Publishing House: Bucharest, Romania, 2009; pp. 442–443 (in Romanian).
4. Sârbu, I.; Ștefan, N.; Oprea A. *Plante vasculare din România. Determinator ilustrat de teren*. 1st ed.; Victor B Victor Publishing House: Bucharest, Romania, 2013; pp. 364–366 (in Romanian).
5. Bi, W.; Gao, Y.; Shen, J.; He, C.; Liu, H.; Peng, Y.; Zhang, C.; Xiao, P. Traditional uses, phytochemistry, and pharmacology of the genus *Acer* (maple): A review. *J. Ethnopharmacol.* **2016**, *189*, 31–60. <https://doi.org/10.1016/j.jep.2016.04.021>.

6. Fan, Y.; Lin, F.; Zhang, R.; Wang, M.; Gu, R.; Long, C. *Acer truncatum* Bunge: A comprehensive review on ethnobotany, phytochemistry and pharmacology. *J. Ethnopharmacol.* **2022**, *282*, 114572. <https://doi.org/10.1016/j.jep.2021.114572>.
7. Şen Utsukarçı, B.; Bal, Y.; Gurdal, B.; Bardakçı Altan, H.; Yılmaz, F.N.; Döşler, S. Pharmacognostical Studies on *Acer campestre* L. subsp. *campestre*. *Int. J. Second. Metab.* **2020**, *7*, 126–138. <https://doi.org/10.21448/ijsm.711952>.
8. Sun, Y.; Yu, R.; Liu, Y.; Liu, J.; Zhang, X.; Gong, Z.; Qu, T. Metabolomics Combined with Transcriptomics Analysis Reveals the Regulation of Flavonoids in the Leaf Color Change of *Acer truncatum* Bunge. *Int. J. Mol. Sci.* **2024**, *25*, 13325. <https://doi.org/10.3390/ijms252413325>.
9. Liu, W.; Ouyang, Y.; Wan, C.P. Flavonoids of the Genus of *Acer*: A Mini Review. *Asian J. Chem.* **2013**, *25*, 7075–7078. <https://doi.org/10.14233/ajchem.2013.14643>.
10. Chang, B.Y.; Jung, Y.S.; Yoon, C.-S.; Oh, J.S.; Hong, J.H.; Kim, Y.-C.; Kim, S.Y. Fraxin Prevents Chemically Induced Hepatotoxicity by Reducing Oxidative Stress. *Molecules* **2017**, *22*, 587. <https://doi.org/10.3390/molecules22040587>.
11. García-Pérez, M.-E.; Kasangana, P.-B.; Stevanovic, T. Bioactive Molecules from *Myrianthus arboreus*, *Acer rubrum*, and *Picea mariana* Forest Resources. *Molecules* **2023**, *28*, 2045. <https://doi.org/10.3390/molecules28052045>.
12. Geoffroy, T.R.; Meda, N.R.; Stevanovic, T. Suitability of DPPH spiking for antioxidant screening in natural products: the example of galloyl derivatives from red maple bark extract. *Anal. Bioanal. Chem.* **2017**, *409*, 5225–5237. <https://doi.org/10.1007/s00216-017-0465-9>.
13. Dong, L.-P.; Ni, W.; Dong, J.-Y.; Li, J.-Z.; Chen, C.-X.; Liu, H.-Y. A New Neolignan Glycoside from the Leaves of *Acer truncatum*. *Molecules* **2006**, *11*, 1009–1014. <https://doi.org/10.3390/11121009>.
14. Aouinti, H.; Touhami, I.; Khouja, M.; Messaoud, C.; Khaldi, A. Chemical composition analysis of seed oil from the three wild Tunisian provenances of *Acer monspessulanum* L. *J. New Sci.* **2022**, *90*, 5106–5112. <https://doi.org/10.55416/sunb.jns01.2211.09004>.
15. Hovanet, M.V.; Dociu, N.; Dinu, M.; Ancuceanu, R.; Morosan, E.; Oprea, E. A Comparative Physico-chemical Analysis of *Acer platanoides* and *Acer pseudoplatanus* Seed Oils. *Rev. Chim. (Bucharest)* **2015**, *66*, 987–991. <https://revistadechimie.ro/Articles.asp?ID=4562> (accessed on 5 December 2024).
16. Le, X.; Zhang, W.; Sun, G.; Fan, J.; Zhu, M. Research on the Differences in Phenotypic Traits and Nutritional Composition of *Acer truncatum* Bunge Seeds from Various Regions. *Foods* **2023**, *12*, 2444. <https://doi.org/10.3390/foods12132444>.
17. Qi, Y.; Huang, Y.; Dong, Y.; Zhang, W.; Xia, F.; Bai, H.; Stevanovic, Z.D.; Li, H.; Shi, L. Effective Improvement of the Oxidative Stability of *Acer truncatum* Bunge Seed Oil, a New Woody Oil Food Resource, by Rosemary Extract. *Antioxidants* **2023**, *12*, 889. <https://doi.org/10.3390/antiox12040889>.
18. Chang, P.; Ma, J.; Xin, H.; Wang, S.; Chen, Z.; Hong, X.; Zhang, B.; Li, L. Comparative Study of the Fatty Acid Composition of the *Acer truncatum* Bunge from Different Producing Areas. *Forests* **2022**, *13*, 1409. <https://doi.org/10.3390/f13091409>.
19. Li, L.; Ma, H.; Liu, T.; Ding, Z.; Liu, W.; Gu, Q.; Mu, Y.; Xu, J.; Seeram, N.P.; Huang, X.; et al. Glucitol-Core Containing Gallotannins-Enriched Red Maple (*Acer rubrum*) Leaves Extract Alleviated Obesity via Modulating Short-Chain Fatty Acid Production in High-Fat Diet-Fed Mice. *J. Funct. Foods* **2020**, *70*, 103970. <https://doi.org/10.1016/j.jff.2020.103970>.
20. Kausar, F.; Farooqi, M.-A.; Farooqi, H.-M.-U.; Salih, A.-R.-C.; Khalil, A.-A.-K.; Kang, C.-w.; Mahmoud, M.H.; Batiha, G.-E.-S.; Choi, K.-h.; Mumtaz, A.-S. Phytochemical Investigation, Antimicrobial, Antioxidant and Anticancer Activities of *Acer cappadocicum* Gled. *Life* **2021**, *11*, 656. <https://doi.org/10.3390/life11070656>.
21. Bhatta, S.; Ratti, C.; Poubelle, P.E.; Stevanovic, T. Nutrients, Antioxidant Capacity and Safety of Hot Water Extract from Sugar Maple (*Acer saccharum* M.) and Red Maple (*Acer rubrum* L.) Bark. *Plant Foods Hum. Nutr.* **2018**, *73*, 25–33. <https://doi.org/10.1007/s11130-018-0656-3>.
22. Meda, N.R.; Poubelle, P.E.; Stevanovic, T. Antioxidant Capacity, Phenolic Constituents and Toxicity of Hot Water Extract from Red Maple Buds. *Chem. Biodivers.* **2017**, *14*, e1700028. <https://doi.org/10.1002/cbdv.201700028>.

23. Yim, N.-H.; Park, E.; Cho, W.-K.; Kim, Y.-H.; Ma, J.Y. Therapeutic Effects of *Acer palmatum* Thumb. Leaf Extract (KIOM-2015E) on Benzalkonium Chloride-Induced Dry Eye in a Mouse Model. *Int. J. Mol. Sci.* **2022**, *23*, 14964. <https://doi.org/10.3390/ijms232314964>.
24. Meda, N.R.; Stevanovic, T.; Poubelle, P.E. Anhydroglucitol-core gallotannins from red maple buds modulate viability of human blood neutrophils. *Toxicol. In Vitro* **2019**, *60*, 76–86. <https://doi.org/10.1016/j.tiv.2019.05.010>.
25. Kim, Y.-H.; Oh, T.W.; Park, E.; Yim, N.-H.; Park, K.I.; Cho, W.K.; Ma, J.Y. Anti-Inflammatory and Anti-Apoptotic Effects of *Acer palmatum* Thumb. Extract, KIOM-2015EW, in a Hyperosmolar-Stress-Induced In Vitro Dry Eye Model. *Nutrients* **2018**, *10*, 282. <https://doi.org/10.3390/nu10030282>.
26. Lee, D.-S.; Cha, B.-Y.; Woo, J.-T.; Kim, Y.-C.; Jang, J.-H. Acerogenin A from *Acer nikoense* Maxim Prevents Oxidative Stress-Induced Neuronal Cell Death through Nrf2-Mediated Heme Oxygenase-1 Expression in Mouse Hippocampal HT22 Cell Line. *Molecules* **2015**, *20*, 12545–12557. <https://doi.org/10.3390/molecules200712545>.
27. Kim, J.H.; Lee, S.; Cho, E.J. The Protective Effects of *Acer okamotoanum* and Isoquercitrin on Obesity and Amyloidosis in a Mouse Model. *Nutrients* **2020**, *12*, 1353. <https://doi.org/10.3390/nu12051353>.
28. Son, S.-Y.; Choi, J.-H.; Kim, E.-B.; Yin, J.; Seonu, S.-Y.; Jin, S.-Y.; Oh, J.-Y.; Lee, M.-W. Chemopreventive Activity of Ellagitannins from *Acer pseudosieboldianum* (Pax) Komarov Leaves on Prostate Cancer Cells. *Plants* **2023**, *12*, 1047. <https://doi.org/10.3390/plants12051047>.
29. Farooqi, H.M.U.; Sammantasinghar, A.; Kausar, F.; Farooqi, M.A.; Chethikkattuveli Salih, A.R.; Hyun, K.; Lim, J.-H.; Khalil, A.A.K.; Mumtaz, A.S.; Choi, K.H. Study of the Anticancer Potential of Plant Extracts Using Liver Tumor Microphysiological System. *Life* **2022**, *12*, 135. <https://doi.org/10.3390/life12020135>.
30. González-Sarrías, A.; Li, L.; Seeram, N.P. Effects of Maple (*Acer*) Plant Part Extracts on Proliferation, Apoptosis and Cell Cycle Arrest of Human Tumorigenic and Non-Tumorigenic Colon Cells. *Phytother. Res.* **2012**, *26*, 995–1002. <https://doi.org/10.1002/ptr.3677>.
31. Nguyen, Q.N.; Lee, S.R.; Kim, B.; Hong, J.-H.; Jang, Y.S.; Lee, D.E.; Pang, C.; Kang, K.S.; Kim, K.H. Estrogenic Activity of 4-Hydroxy-Benzoic Acid from *Acer tegmentosum* via Estrogen Receptor  $\alpha$ -Dependent Signaling Pathways. *Plants* **2022**, *11*, 3387. <https://doi.org/10.3390/plants11233387>.
32. Lee, S.R.; Park, Y.J.; Han, Y.B.; Lee, J.C.; Lee, S.; Park, H.-J.; Lee, H.-J.; Kim, K.H. Isoamericanic Acid B from *Acer tegmentosum* as a Potential Phytoestrogen. *Nutrients* **2018**, *10*, 1915. <https://doi.org/10.3390/nu10121915>.
33. Ha, H.; Shim, K.-S.; Kim, T.; An, H.; Lee, C.-J.; Lee, K.J.; Ma, J.Y. Water Extract of *Acer tegmentosum* Reduces Bone Destruction by Inhibiting Osteoclast Differentiation and Function. *Molecules* **2014**, *19*, 3940–3954. <https://doi.org/10.3390/molecules19043940>.
34. Phong, N.V.; Min, B.S.; Yang, S.Y.; Kim, J.A. Inhibitory Effect of Coumarins and Isocoumarins Isolated from the Stems and Branches of *Acer mono* Maxim. against *Escherichia coli*  $\beta$ -Glucuronidase. *Appl. Sci.* **2022**, *12*, 10685. <https://doi.org/10.3390/app122010685>.
35. Zhang, X.-Y.; Liu, Y.-H.; Liu, D.-Z.; Xu, J.-Y.; Zhang, Q. Insulin-Mimic Components in *Acer truncatum* Leaves: Bio-Guided Isolation, Annual Variance Profiling and Regulating Pathway Investigated by Omics. *Pharmaceuticals* **2021**, *14*, 662. <https://doi.org/10.3390/ph14070662>.
36. Liang, Y.; Kong, F.; Ma, X.; Shu, Q. Inhibitory Effect of *Acer truncatum* Bunge Seed Coat Extract on Fatty Acid Synthase, Differentiation and Lipid Accumulation in 3T3-L1 Adipocytes. *Molecules* **2022**, *27*, 1324. <https://doi.org/10.3390/molecules27041324>.
37. Cho, H.-H.; Lee, S.-J.; Kim, S.-H.; Jang, S.-H.; Won, C.; Kim, H.-D.; Kim, T.H.; Cho, J.-H. *Acer tegmentosum* Maxim Inhibits Adipogenesis in 3t3-L1 Adipocytes and Attenuates Lipid Accumulation in Obese Rats Fed a High-Fat Diet. *Nutrients* **2020**, *12*, 3753. <https://doi.org/10.3390/nu12123753>.
38. Kim, J.H.; Lee, S.; Cho, E.J. Flavonoids from *Acer okamotoanum* Inhibit Adipocyte Differentiation and Promote Lipolysis in the 3T3-L1 Cells. *Molecules* **2020**, *25*, 1920. <https://doi.org/10.3390/molecules25081920>.
39. Ma, H.; Xu, J.; DaSilva, N.A.; Wang, L.; Wei, Z.; Guo, L.; Johnson, S.L.; Lu, W.; Xu, J.; Gu, Q.; Seeram, N.P. Cosmetic applications of glucitol-core containing gallotannins from a proprietary phenolic-enriched red maple (*Acer rubrum*) leaves extract: inhibition of melanogenesis via down-regulation of tyrosinase and melanogenic gene expression in B16F10 melanoma cells. *Arch. Dermatol. Res.* **2017**, *309*, 265–274. <https://doi.org/10.1007/s00403-017-1728-1>.

40. Li, H.; Roy, T.; Boateng, S.T.; He, H.; Liu, C.; Liu, W.; Li, D.; Wu, P.; Seeram, N.P.; Chamcheu, J.C.; et al. Standardized Pomegranate (Pomella®) and Red Maple (Maplifa®) Extracts and Their Phenolics Protect Type I Collagen by the Inhibition of Matrix Metalloproteinases, Collagenase, and Collagen Cross-Linking. *Molecules* **2022**, *27*, 7919. <https://doi.org/10.3390/molecules27227919>.
41. Jin, Y.-J.; Ji, Y.; Jang, Y.-P.; Choung, S.-Y. *Acer tataricum* subsp. *ginnala* Inhibits Skin Photoaging via Regulating MAPK/AP-1, NF- $\kappa$ B, and TGF $\beta$ /Smad Signaling in UVB-Irradiated Human Dermal Fibroblasts. *Molecules* **2021**, *26*, 662. <https://doi.org/10.3390/molecules26030662>.
42. Ma, H.; Guo, H.; Liu, C.; Wan, Y.; Seeram, N.P. Protective Effects of a Red Maple (*Acer rubrum*) Leaves Extract on Human Keratinocytes against H<sub>2</sub>O<sub>2</sub>-induced Oxidative Stress. *FASEB J.* **2018**, *32*, 656.33–656.33. [https://doi.org/10.1096/fasebj.2018.32.1\\_supplement.656.33](https://doi.org/10.1096/fasebj.2018.32.1_supplement.656.33).
43. Liu, J.; Liang, S.; Qin, K.; Jia, B.; Ren, Z.; Yang, X.; Yang, X. *Acer truncatum* leaves extract modulates gut microbiota, improves antioxidant capacity, and alleviates lipopolysaccharide-induced inflammation in broilers. *Poult. Sci.* **2023**, *102*, 102951. <https://doi.org/10.1016/j.psj.2023.102951>.
44. Chen, X.; Song, Y.; Song, W.; Han, J.; Cao, H.; Xu, X.; Li, S.; Fu, Y.; Ding, C.; Lin, F.; Shi, Y.; Li, J. Multi-omics reveal neuroprotection of *Acer truncatum* Bunge Seed extract on hypoxic-ischemia encephalopathy rats under high-altitude. *Commun. Biol.* **2023**, *6*, 1001. <https://doi.org/10.1038/s42003-023-05341-9>.
45. Chen, X.; Song, W.; Song, Y.; Cao, H.; Xu, X.; Li, S.; Fu, Y.; Xue, T.; Ding, C.; Lin, F.; Shi, Y.; Li, J. Lipidomics reveal the cognitive improvement effects of *Acer truncatum* Bunge seed oil on hypoxic-ischemic encephalopathy rats. *Food Funct.* **2023**, *14*, 6610–6623. <https://doi.org/10.1039/D3FO01583A>.
46. Song, W.; Zhang, K.; Xue, T.; Han, J.; Peng, F.; Ding, C.; Lin, F.; Li, J.; Sze, F.T.A.; Gan, J.; Chen, X. Cognitive improvement effect of nervonic acid and essential fatty acids on rats ingesting *Acer truncatum* Bunge seed oil revealed by lipidomics approach. *Food Funct.* **2022**, *13*, 2475–2490. <https://doi.org/10.1039/d1fo03671h>.
47. Mohsenpour, H.; Pesce, M.; Patrino, A.; Bahrami, A.; Pour, P.M.; Farzaei, M.H. A Review of Plant Extracts and Plant-Derived Natural Compounds in the Prevention/Treatment of Neonatal Hypoxic-Ischemic Brain Injury. *Int. J. Mol. Sci.* **2021**, *22*, 833. <https://doi.org/10.3390/ijms22020833>.
48. Bi, W.; Shen, J.; Gao, Y.; He, C.; Peng, Y.; Xiao, P. Ku-jin tea (*Acer tataricum* subsp. *ginnala* or *A. tataricum* subsp. *theiferum*), an underestimated functional beverage rich in antioxidant phenolics. *J. Funct. Foods* **2016**, *24*, 75–84. <https://doi.org/10.1016/j.jff.2016.04.002>.
49. El-Khatib, A.H.; Engel, A.M.; Weigel, S. Co-Occurrence of Hypoglycin A and Hypoglycin B in Sycamore and Box Elder Maple Proved by LC-MS/MS and LC-HR-MS. *Toxins* **2022**, *14*, 608. <https://doi.org/10.3390/toxins14090608>.
50. Renaud, B.; Kruse, C.-J.; François, A.-C.; Grund, L.; Bunert, C.; Brisson, L.; Boemer, F.; Gault, G.; Ghislain, B.; Petitjean, T.; et al. *Acer pseudoplatanus*: A Potential Risk of Poisoning for Several Herbivore Species. *Toxins* **2022**, *14*, 512. <https://doi.org/10.3390/toxins14080512>.
51. Kamiński, P.; Gruba, M.; Fekner, Z.; Tyśkiewicz, K.; Kobus, Z. The Influence of Water Extraction Parameters in Subcritical Conditions and the Shape of the Reactor on the Quality of Extracts Obtained from Norway Maple (*Acer platanoides* L.). *Processes* **2023**, *11*, 3395. <https://doi.org/10.3390/pr11123395>.
52. Zhang, M.; Choe, J.; Bu, T.; Liu, S.; Kim, S. Comparison of Antioxidant Properties and Metabolite Profiling of *Acer pseudoplatanus* Leaves of Different Colors. *Antioxidants* **2023**, *12*, 65. <https://doi.org/10.3390/antiox12010065>.
53. Kim, I.; Ha, J.-H.; Jeong, Y. Optimization of Extraction Conditions for Antioxidant Activity of *Acer tegmentosum* Using Response Surface Methodology. *Appl. Sci.* **2021**, *11*, 1134. <https://doi.org/10.3390/app11031134>.
54. Atroune, F.; Chaker, S.; Djebbar, R.; Dahmani-Megrerouche, M. Comparative evaluation of phenolics content and antioxidant activity of leaves and branches of field maple (*Acer campestre*) from two populations of Northeastern Algeria. *An. Univ. Oradea Fasc. Biol.* **2019**, *XXVI*, 7–13. <https://www.bioresearch.ro/2019-1.html> (accessed on 5 December 2024).

55. Yang, L.; Yin, P.; Fan, H.; Xue, Q.; Li, K.; Li, X.; Sun, L.; Liu, Y. Response Surface Methodology Optimization of Ultrasonic-Assisted Extraction of *Acer truncatum* Leaves for Maximal Phenolic Yield and Antioxidant Activity. *Molecules* **2017**, *22*, 232. <https://doi.org/10.3390/molecules22020232>.
56. Meng, R.; Ou, K.; Chen, L.; Jiao, Y.; Jiang, F.; Gu, R. Response Surface Optimization of Extraction Conditions for the Active Components with High Acetylcholinesterase Inhibitory Activity and Identification of Key Metabolites from *Acer truncatum* Seed Oil Residue. *Foods* **2023**, *12*, 1751. <https://doi.org/10.3390/foods12091751>.

**Disclaimer/Publisher's Note:** The statements, opinions and data contained in all publications are solely those of the individual author(s) and contributor(s) and not of MDPI and/or the editor(s). MDPI and/or the editor(s) disclaim responsibility for any injury to people or property resulting from any ideas, methods, instructions or products referred to in the content.